

An Online Learned CRF Model for Multi-Target Tracking

Bo Yang and Ram Nevatia

Institute for Robotics and Intelligent Systems, University of Southern California
Los Angeles, CA 90089, USA

{yangbo|nevatia}@usc.edu

Abstract

We introduce an online learning approach for multi-target tracking. Detection responses are gradually associated into tracklets in multiple levels to produce final tracks. Unlike most previous approaches which only focus on producing discriminative motion and appearance models for all targets, we further consider discriminative features for distinguishing difficult pairs of targets. The tracking problem is formulated using an **online learned CRF model**, and is transformed into an energy minimization problem. The energy functions include a set of unary functions that are based on motion and appearance models for discriminating all targets, as well as a set of pairwise functions that are based on models for differentiating corresponding pairs of tracklets. The online CRF approach is more powerful at distinguishing spatially close targets with similar appearances, as well as in dealing with camera motions. An efficient algorithm is introduced for finding an association with low energy cost. We evaluate our approach on three public data sets, and show significant improvements compared with several state-of-art methods.

1. Introduction

Tracking multiple targets is an important but difficult problem in computer vision. It aims at finding trajectories of all targets while maintaining their identities. Due to great improvements on object detection, association based tracking approaches have been proposed [11, 17, 2, 12, 18]. They often find proper linking affinities based on multiple cues between detection responses or tracklets, *i.e.*, track fragments, and find a global solution with maximum probability using Hungarian algorithm, MCMC, etc.

Association based approaches are powerful at dealing with extended occlusions between targets and the complexity is polynomial in the number of targets. However, how to better distinguish different targets remains a key issue that limits the performance of association based tracking. It is difficult to find descriptors to distinguish targets in crowded scenes with frequent occlusions and similar appearances. In this paper, we propose an online learned condition random



Figure 1. Examples of tracking results by our approach.

field (CRF) model to better discriminating different targets, especially difficult pairs, which are spatially near targets with similar appearance. Figure 1 shows some tracking examples by our approach.

To identify each target, motion and appearance information are often adopted to produce discriminative descriptors. Motion descriptors are often based on speeds and distances between tracklet pairs, while appearance descriptors are often based on global or part based color histograms to distinguish different targets.

In most previous association based tracking work, appearance models are pre-defined [17, 12] or online learned to discriminate all targets [7, 13] or to discriminate one target with all others [3, 8]. Though such learned appearance models are able to distinguish most targets, they are not necessarily capable of differentiating difficult pairs, *i.e.*, close targets with similar appearances. The discriminative features between a difficult pair are possibly quite different with those for distinguishing with all other targets.

Linear motion models are widely used in previous tracking work [15, 19, 3]; linking probabilities between tracklets are often based on how well a pair of tracklets satisfies a linear motion assumption. However, as shown in the first row of Figure 2, if the view angle changes due to camera

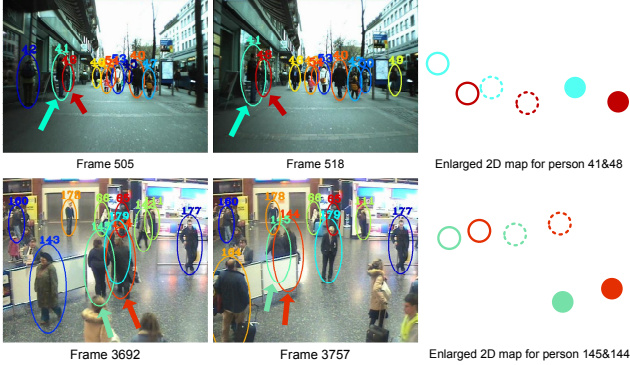


Figure 2. Examples of relative positions and linear estimations. In the 2D map, filled circles indicate positions of person at the earlier frames; dashed circles and solid circles indicate estimated positions by linear motion models and real positions at the later frames respectively.

motion, the motion smoothness would be impaired; it could be compensated by frame matching techniques, but this is a challenging task by itself. Relative positions between targets are less dependent on view angles, and are often more stable than linear motion models for dealing with camera motions. For static cameras, relative positions are still helpful, as shown in the second row of Figure 2; some targets may not follow a linear motion model, and relative positions between neighboring targets are useful for recovering errors in a linear motion model.

Based on above observations, we propose an online learning approach, which formulates the multi-target tracking problem as inference in a conditional random field (CRF) model as shown in Figure 3. Our CRF framework incorporates global models for distinguishing all targets and pairwise models for differentiating difficult pairs of targets.

All linkable tracklet pairs form the nodes in this CRF model, and labels of each node (1 or 0) indicate whether two tracklets can be linked or not. The energy cost for each node is estimated based on global appearance and motion models similar to [7]. The energy cost for an edge is based on discriminative pairwise models, *i.e.*, appearance and motion descriptors, that are online learned for distinguishing tracklets in the connected two CRF nodes. Global models and pairwise models are used to produce unary and pairwise energy functions respectively, and the tracking problem is transformed into an energy minimization task.

The contributions of this paper are:

- A CRF framework for modeling both global tracklets affinity models and pairwise discriminative models.
- An online learning approach for producing unary and pairwise energy functions in a CRF model.
- An approximation algorithm for efficiently finding good tracking solutions with low energy costs.

The rest of the paper is organized as follows: related work is discussed in Section 2; problem formulation is

given in Section 3; Section 4 describes the online learning approach for a CRF model; experiments are shown in Section 5, followed by conclusion in Section 6.

2. Related Work

Multi-target tracking has been an important topic in computer vision for several years. One key issue in tracking is that how to distinguish targets with backgrounds and with each other.

Most visual tracking methods focus on tracking single object or multiple objects separately [9, 16]; they usually try to find proper appearance models that distinguish one object with all other targets or backgrounds, and adopt meanshift [4] or particle filtering [6] like approach to online adjust target appearance models, and use updated models to continuously track targets.

On the other hand, most association based methods focus on tracking multiple objects of a pre-known class simultaneously [11, 14, 2, 18]. They usually associate detection responses produced by a pre-trained detector into long tracks, and find a global optimal solution for all targets. Appearance models are often pre-defined [17, 12] or online learned to distinguish multiple targets globally [13, 7]; in addition, linear motion models between tracklet pairs [15, 3] are often adopted to constrain motion smoothness. Though such approaches may obtain global optimized appearance and motion models, they are not necessarily able to differentiate difficult pairs of targets, *i.e.*, close ones with similar appearances, as appearance models for distinguishing a specific pair of targets may be quite different with those used for distinguishing all targets, and previous motion models are not stable for non-static cameras. However, our online CRF models consider both global and pairwise discriminative appearance and motion models.

Note that CRF models are also adopted in [19]. Both [19] and this approach relax the assumption that associations between tracklet pairs are independent of each other. However, [19] focused on modeling association dependencies, while this approach aims at better distinction between difficult pairs of targets and therefore the meanings of edges in CRF are different. In addition, [19] is an offline approach that integrates multiple cues on pre-labeled ground truth data, but our approach is an online learning method that finds discriminative models automatically without pre-labeled data.

3. CRF Formulation for Tracking

Given a video input, we first detect targets in each frame by a pre-trained detector. Similar to [7], we adopt a low level association process to connect detection responses in neighboring frames into reliable tracklets, and then associate the tracklets progressively in multiple levels. A tracklet $T_i = \{d_i^{t_i^s}, \dots, d_i^{t_i^e}\}$ is defined as a set of detection or interpolated responses in consecutive frames, where t_i^s and t_i^e

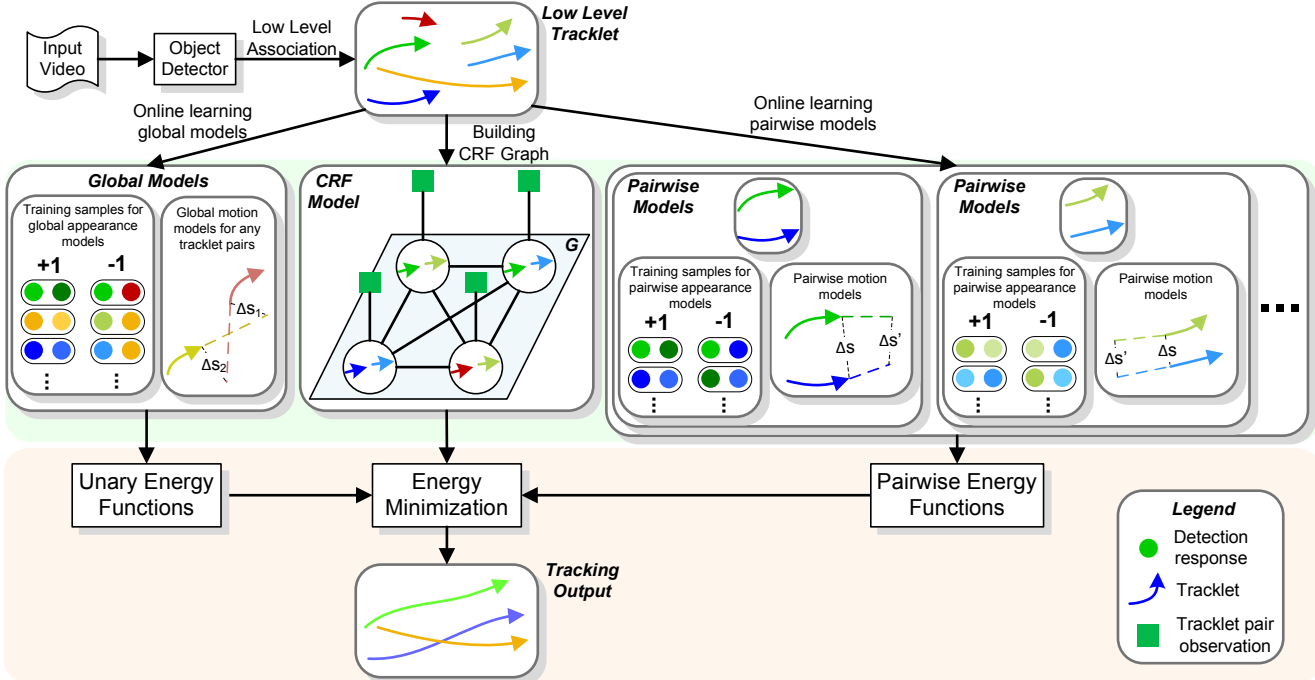


Figure 3. Tracking framework of our approach. In the CRF model, each node denotes a possible link between a tracklet pair and has a unary energy cost based on global appearance and motion models; each edge denotes a correlation between two nodes and has a pairwise energy cost based on discriminative appearance and motion models specifically for the two nodes. Colors of detection responses indicate their belonging tracklets. Best viewed in color.

denote the start and end frames of T_i and $d_i^t = \{p_i^t, s_i^t, v_i^t\}$ denote the response at frame t , including position p_i^t , size s_i^t , and velocity vector v_i^t .

At each level, the input is the set of tracklets produced in previous level $S = \{T_1, T_2, \dots, T_n\}$. For each possible association pair of tracklet ($T_{i_1} \rightarrow T_{i_2}$), we introduce a label l_i , where $l_i = 1$ indicates T_{i_1} is linked to T_{i_2} , and $l_i = 0$ indicates the opposite. We aim to find the best set of associations with the highest probability. We formulate the tracking problem as finding the best L given S

$$L^* = \underset{L}{\operatorname{argmax}} P(L|S) = \underset{L}{\operatorname{argmax}} \frac{1}{Z} \exp(-\Psi(L|S)) \quad (1)$$

where Z is a normalization factor, and Ψ is a cost function. Assuming that the joint distributions for more than two associations do not make contributions to $P(L|S)$, we have

$$\begin{aligned} L^* &= \underset{L}{\operatorname{argmin}} \Psi(L|S) \\ &= \underset{L}{\operatorname{argmin}} \sum_i U(l_i|S) + \sum_{ij} B(l_i, l_j|S) \end{aligned} \quad (2)$$

where $U(l_i|S) = -\ln P(l_i|S)$ and $B(l_i, l_j|S) = -\ln P(l_i, l_j|S)$ denote the unary and pairwise energy functions respectively. In Equ. 2, the first part defines the linking probabilities between any two tracklets based on global appearance and motion models, while the second part defines the correlations between tracklet pairs based on discriminative models especially learned for corresponding pairs of tracklets.

We model the tracking problem by a Conditional Random Field (CRF) model. As shown in Figure 3, a graph $G = (V, E)$ is created for each association level, where $V = \{v_1, \dots, v_p\}$ denotes the set of nodes, and $E = \{e_1, \dots, e_q\}$ denotes the set of edges. Each node $v_i = (T_{i_1} \rightarrow T_{i_2})$ denotes a possible association between tracklets T_{i_1} and T_{i_2} ; each edge $e_j = \{(v_{j_1}, v_{j_2})\}$ denotes a correlation between two nodes. A label $L = \{l_1, \dots, l_p\}$ on V denotes an association result for current level. We assume that one tracklet cannot be associated with more than one tracklet, and therefore any valid label set L should satisfy

$$\sum_{v_i \in \text{Head}_{i_1}} l_i \leq 1 \quad \& \quad \sum_{v_i \in \text{Tail}_{i_2}} l_i \leq 1 \quad (3)$$

$$\text{Head}_{i_1} = \{(T_{i_1} \rightarrow T_j) \in V\} \quad \forall T_j \in S$$

$$\text{Tail}_{i_2} = \{(T_j \rightarrow T_{i_2}) \in V\} \quad \forall T_j \in S$$

where the first constraint limits any tracklet T_{i_1} link to at most one other tracklet, and the second constraint limits that at most one tracklet may be link to any tracklet T_{i_2} .

For efficiency, we track in sliding windows one by one instead of processing the whole video at one time. The CRF models are learned individually in each sliding window.

4. Online Learning of CRF Models

In this section, we introduce our tracking approach in several steps, including CRF graph creation, online learn-



Figure 4. Examples of head close and tail close tracklet pairs.

ing of unary and pairwise terms, as well as how to find an association label set with low energy.

4.1. CRF Graph Creation for Tracklets Association

Given a set of tracklets $S = \{T_1, T_2, \dots, T_n\}$ as input, we want to create a CRF graph for modeling all possible associations between tracklets and their correlations. Tracklet T_i is linkable to T_j if the gap between the end of T_i and the beginning of T_j satisfies

$$0 < t_j^s - t_i^e < t_{max} \quad (4)$$

where t_{max} is a threshold for maximum gap between any linkable pair of tracklets, and t_j^s and t_i^e denotes the start and end frames of T_j and T_i respectively. We create the set of nodes V in CRF to modeling all linkable tracklets as

$$V = \{v_i = (T_{i_1} \rightarrow T_{i_2})\} \text{ s.t. } T_{i_1} \text{ is linkable to } T_{i_2} \quad (5)$$

Instead of modeling association dependencies as in [19], edges in our CRF provide corresponding pairwise models between spatially close targets, and are defined between any nodes that have *tail close* or *head close* tracklet pairs.

As shown in Figure 4, two tracklets T_i and T_j are a *head close* pair if they satisfy (suppose $t_j^s \geq t_i^s$)

$$t_i^s < t_j^e \text{ & } \|p_i^{t_i^s} - p_j^{t_j^s}\| < \gamma \min\{s_i^{t_i^s}, s_j^{t_j^s}\} \quad (6)$$

where γ is a distance control factor, set to 3 in our experiments. This definition indicates that the head part of T_i is close to T_j at T_i 's beginning frame. The definition of *tail close* is similar.

Then we define the set of edges E as

$$E = \{(v_i, v_j)\} \quad \forall v_i, v_j \in V \quad (7)$$

s.t. T_{i_1} and T_{j_1} are tail close, or T_{i_2} and T_{j_2} are head close.

Such definition constraints the edges on difficult pairs where wrong associations are most likely to happen, so that edges produce proper pairwise energies to distinguish them.

4.2. Learning of Unary Terms

Unary terms in Equ. 2 define the energy cost for associating pairs of tracklets. As defined in section 3, $U(l_i|S) = -\ln P(l_i|S)$. We further divide the probability into motion based probability $P_m(\cdot)$ and appearance based probability $P_a(\cdot)$ as

$$U(l_i = 1|S) = -\ln(P_m(T_{i_1} \rightarrow T_{i_2}|S)P_a(T_{i_1} \rightarrow T_{i_2}|S)) \quad (8)$$

P_m is defined as in [7, 19, 8], which is based on the distance between estimations of positions based on linear motion models and the real positions. As shown in Figure 5, the motion probability between tracklets T_1 and T_2

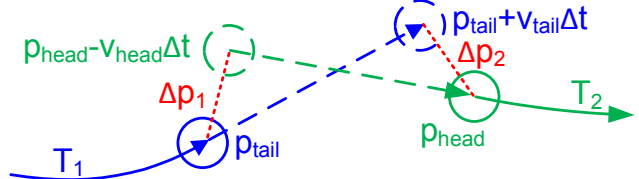


Figure 5. Global motion models for unary terms in CRF.

are defined based on $\Delta p_1 = p^{head} - v^{head} \Delta t - p^{tail}$ and $\Delta p_2 = p^{tail} + v^{tail} \Delta t - p^{head}$ as

$$P_m(T_{i_1} \rightarrow T_{i_2}|S) = G(\Delta p_1, \Sigma_p)G(\Delta p_2, \Sigma_p) \quad (9)$$

where $G(\cdot, \Sigma)$ is the zero-mean Gaussian function, and Δt is the frame difference between p^{tail} and p^{head} .

For $P_a(\cdot)$, we adopt the online learned discriminative appearance models (OLDAMs) defined in [7], which focus on learning appearance models with good global discriminative abilities between targets.

4.3. Learning of Pairwise Terms

Similar to unary terms, pairwise terms are also decomposed into motion based and appearance based parts. Motion based probabilities are defined based on relative distance between tracklet pairs. Take two nodes (T_1, T_3) and (T_2, T_4) as an example. Suppose T_1 and T_2 are a tail close pair; therefore, there is an edge between the two nodes. Let $t_x = \min\{t_1^e, t_2^e\}$, and $t_y = \max\{t_1^s, t_4^s\}$.

As T_1 and T_2 are tail close, we estimate positions of both at frame t_y , as shown in dash circles in Figure 6. Then we can get the estimated relative distance between T_1 and T_2 at frame t_y as

$$\Delta p_1 = (p_1^{t_1^e} + V_1^{tail}(t_y - t_1^e)) - (p_2^{t_2^e} + V_2^{tail}(t_y - t_2^e)) \quad (10)$$

where V_1^{tail} and t_1^e are the tail velocity and end frames of T_1 ; V_2^{tail} and t_2^e are similar. We compare the estimated relative distance with the real one Δp_2 , and use the same Gaussian function in Equ. 9 to compute the pairwise motion probability as $G(\Delta p_1 - \Delta p_2, \Sigma_p)$.

As shown in Figure 6, the difference between Δp_1 and Δp_2 is small. This indicates that if T_1 is associated to T_3 , there is a high probability that T_2 is associated to T_4 and vice versa. Note that if T_3 and T_4 in Figure 6 are head close, we also do a similar computation as above; the final motion probability would be taken as the average of both.

Pairwise appearance models are designed for differentiating specific close pairs. For example, in Figure 6, T_1 and T_2 are a tail close pair; we want to produce an appearance model that best distinguishes the two targets without considering other targets or backgrounds.

Therefore, we online collect positive and negative samples only from the concerned two tracklets so that the learned appearance models are most discriminative for these two. Positive samples are selected from responses in the same tracklet; any pair of these responses should have

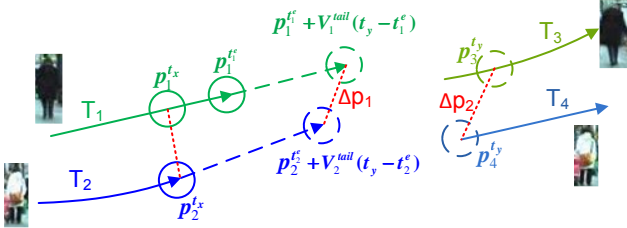


Figure 6. Pairwise motion models for pairwise terms in CRF.

high appearance similarity. For a tail close tracklet pair T_1 and T_2 , the positive sample set \mathbb{S}^+ is defined as

$$\begin{aligned}\mathbb{S}^+ &= \{(d_k^{t_1}, d_k^{t_2})\} \quad k \in \{1, 2\} \\ \forall t_1, t_2 &\in [\max\{t_k^s, t_k^e - \theta\}, t_k^e]\end{aligned}\quad (11)$$

where θ is a threshold for the number of frames used for computing appearance models (set to 10 in our experiments). The introduction of θ is because a target may change appearance a lot after some time due to illumination, view angle, or pose changes.

Negative samples are selected from responses in different tracklets, and they should have as much differences as possible in appearance. The negative sample set \mathbb{S}^- between T_1 and T_2 is defined as

$$\mathbb{S}^- = \{(d_1^{t_1}, d_2^{t_2})\} \quad (12)$$

$$\forall t_1 \in [\max\{t_1^s, t_1^e - \theta\}, t_1^e], \quad \forall t_2 \in [\max\{t_2^s, t_2^e - \theta\}, t_2^e]$$

Sample collection for head close pairs are similar, but detection responses are from the first θ frames of each tracklet.

With the positive and negative sample sets, we adopt the standard Real Boost algorithm to produce appearance models for best distinguishing T_1 and T_2 ; we adopt the features defined in [7], including color, texture, and shape for different regions of targets. Based on the pairwise model, we get new appearance based probabilities for (T_1, T_3) and (T_2, T_4) shown in Figure 6. If T_3 and T_4 are a head close pair, we adopt a similar learning approach to get appearance probabilities based on discriminative models for T_3 and T_4 , and use the average of both scores as the final pairwise appearance probabilities.

Note that the discriminative appearance models between T_1 and T_2 are only learned once for all edges like $\{(T_1, T_x), (T_2, T_y)\} \quad \forall T_x, T_y \in S$. Therefore, the complexity is much less than the number of edges and becomes $O(n^2)$, where n is the number of tracklets. Moreover, as only a few tracklet pairs are likely to be spatially close, the actual times of learning is often much smaller than n^2 .

4.4. Energy Minimization

For CRF models with submodular energy functions, where $B(0, 0) + B(1, 1) < B(1, 0) + B(1, 1)$, a global optimal solution can be found by the graph cut algorithm. However, due to the constraints in Equ. 3, the energy function in our formulation is not sub-modular. Therefore, it is difficult to find the global optimal solution in polynomial

time. Instead, we introduce a heuristic algorithm to find a good solution in polynomial time.

The unary terms in our CRF model have been shown to be effective for non-difficult pairs by previous work [7]. Considering this issue, we first use the Hungarian algorithm [11] to find a global optimal solution by only considering the unary terms and satisfying the constraints in Equ. 3. Then we sort the selected associations, *i.e.*, nodes with labels of 1, according to their unary term energies from least to most as $A = \{v_i = (T_{i_1} \rightarrow T_{i_2})\}$. Then for each selected node, we try to switch labels of it and each neighboring node, *i.e.*, a node that is connected with current node by an edge in the CRF model; if the energy is lower, we keep the change. The energy minimization algorithm is shown in Algorithm 1.

Algorithm 1 Finding labels with low energy cost.

Input: Tracklets from previous level $S = \{T_1, T_2, \dots, T_n\}$; CRF graph $G = (V, E)$.

Find the label set L with the lowest unary energy cost by Hungarian algorithm, and evaluate its overall energy Ψ by Equ. 2.

Sort nodes with labels of 1 according to their unary energy costs from least to most as $\{v_1, \dots, v_k\}$.

For $i = 1, \dots, k$ **do**:

- Set updated energy $\Psi' = +\infty$
- **For** $j = 1, \dots, t$ that $(v_i, v_j) \in E$ **do**:
- Switch labels of l_i and l_j under constraints in Equ. 3, and evaluate new energy Ω .
- If $\Omega < \Psi'$, $\Psi' = \Omega$
- If $\Psi' < \Psi$, update L with the switch, and set $\Psi = \Psi'$.

Output: The set of labels L on the CRF graph.

Note that the Hungarian algorithm has a complexity of $O(n^3)$, while our heuristic search process has a complexity of $O(|E|) = O(n^4)$. Therefore, the overall complexity is still polynomial. In addition, as nodes are only defined between tracklets with a proper time gap and edges are only defined between nodes with head or tail close tracklet pair, the actual number of edges is typically much smaller than n^4 . In our experiments, the run time is almost linear in the number of targets.

5. Experiments

We evaluate our approach on three public pedestrian data sets: the TUD data set [2], Trecvid 2008 [1], and ETH mobile pedestrian [5] data set. We show quantitative comparisons with state-of-art methods, as well as visualized results of our approach. Though frame rates, resolutions and densities are different in these data sets, we use the same parameter setting, and performance improves compared to previous methods for all of them. This indicates that our approach has low sensitivity on parameters. All data used in our experiments are publicly available¹.

¹<http://iris.usc.edu/people/yangbo/downloads.html>

Method	Recall	Precision	FAF	GT	MT	PT	ML	Frag	IDS
Energy Minimization [2]	-	-	-	9	60.0%	30.0%	0.0%	4	7
PRIMPT [8]	81.0%	99.5%	0.028	10	60.0%	30.0%	10.0%	0	1
Online CRF Tracking	87.0%	96.7%	0.184	10	70.0%	30.0%	0.0%	1	0

Table 1. Comparison of results on TUD dataset. The PRIMPT results are provided by courtesy of authors of [8]. Our ground truth includes all persons appearing in the video, and has one more person than that in [2].

Method	Recall	Precision	FAF	GT	MT	PT	ML	Frag	IDS
Offline CRF Tracking [19]	79.2%	85.8%	0.996	919	78.2%	16.9%	4.9%	319	253
OLDAMs [7]	80.4%	86.1%	0.992	919	76.1%	19.3%	4.6%	322	224
PRIMPT [8]	79.2%	86.8%	0.920	919	77.0%	17.7%	5.2%	283	171
Online CRF Tracking	79.8%	87.8%	0.857	919	75.5%	18.7%	5.8%	240	147

Table 2. Comparison of tracking results on Trecvid 2008 dataset. The human detection results are the same as used in [19, 7, 8], and are provided by courtesy of authors of [8].

5.1. Evaluation Metric

As it is difficult to use a single score to evaluate tracking performance, we adopt the evaluation metric defined in [10], including:

- **Recall(\uparrow):** correctly matched detections / total detections in ground truth.
- **Precision(\uparrow):** correctly matched detections / total detections in the tracking result.
- **FAF(\downarrow):** Average false alarms per frame.
- **GT:** The number of trajectories in ground truth.
- **MT(\uparrow):** The ratio of mostly tracked trajectories, which are successfully tracked for more than 80%.
- **ML(\downarrow):** The ratio of mostly lost trajectories, which are successfully tracked for less than 20%.
- **PT:** The ratio of partially tracked trajectories, *i.e.*, $1 - MT - ML$.
- **Frag(\downarrow):** fragments, the number of times that a ground truth trajectory is interrupted.
- **IDS(\downarrow):** id switch, the number of times that a tracked trajectory changes its matched id.

For items with \uparrow , higher scores indicate better results; for those with \downarrow , lower scores indicate better results.

5.2. Results on Static Camera Videos

We first test our results on data sets captured by static cameras, *i.e.*, TUD [2] and Trecvid 2008 [1].

For fair comparison, we use the same TUD-Stadtmitte data set as used in [2]. It is captured on a street at a very low camera angle, and there are frequent full occlusions among pedestrians. But the video is quite short, and contains only 179 frames.

The quantitative results are shown in Table 1. We can see that our results are much better than that in [2], but the improvement is not so obvious compared with [8]: we have higher MT and recall and lower id switches, but PRIMPT

has higher precision and lower fragments. This is because the online CRF model focuses on better differentiating difficult pairs of targets, but there are not many people in the TUD data set. Some visual results are shown in the first row of Figure 7; our approach is able to keep correct identities while targets are quite close, such as person 0, person 1, and person 2.

To see the effectiveness of our approach, we further evaluate our approach on the difficult Trecvid 2008 data set. There are 9 video clips in the data set, each of which has 5000 frames; these videos are captured in a busy airport, and have high density of people with frequent occlusions. There are lots of close track interactions in this data set, indicating huge number of edges in the CRF graph. The comparison results are shown in Table 2. Compared with up-to-date approaches, our online CRF achieves best performance on precision, FAF, fragments, and id switches, while keeping recall and MT competitive. Compared with [8], our approach reduces the fragments and the id switches by about 15% and 14% respectively. Row 2 and 3 in Figure 7 show some tracking examples by our approach. We can see that when targets with similar appearances get close, the online CRF can still find discriminative features to distinguish these difficult pairs. However, global appearance and motion models are not effective enough in such cases, such as person 106 and 109 in the third row of Figure 7, who are both in white, move in similar directions, and are quite close. The second row in Figure 2 shows an example where the approach in [7] produces a fragmentation due to non-linear motions while our approach has no fragments by considering pairwise terms in the CRF model.

5.3. Results on Moving Camera Videos

We further evaluate our approach on the ETH data set [5], which is captured by a pair of cameras on a moving stroller in busy street scenes. The stroller is mostly moving forward, but sometimes has panning motions, which makes

the motion affinity between two tracklets less reliable.

For fair comparison, we choose the “BAHNHOF” and “SUNNY DAY” sequences used in [8] for evaluation. They have 999 and 354 frames respectively, and people are under frequent occlusions due to the low view angles of cameras. For fair comparison with [8], we also use the sequence from the left camera; no depth and ground plane information are used.

The quantitative results are shown in Table 3. We can see that our approach achieves better or the same performances on all evaluation scores. The mostly tracked score is improved by about 10%; fragments are reduced by 17%; recall and precision are improved by about 2% and 4% respectively. The obvious improvement in MT and fragment scores indicate that our approach can better track targets under moving cameras, where the traditional motion models are less reliable.

The last two rows in Figure 7 show some visual tracking results by our online CRF approach. Both examples show obvious panning movements of cameras. Traditional motion models, *i.e.*, unary motion models in our online CRF, would produce low affinity scores for tracklets belonging to the same targets. However, by considering pairwise terms, relative positions are helpful for connecting correct tracklets into one. This explains the obvious improvements on MT and fragments. The first row in Figure 2 shows an example that our approach successfully tracks persons 41 and 48 under abrupt camera motions, while the method in [7] fails to find the correct associations.

5.4. Speed

As discussed in Section 4.4, the complexity of our algorithm is polynomial in the number of tracklets. Our experiments are performed on a Intel 3.0GHz PC with 8G memory, and the codes are implemented in C++. For the less crowded TUD and ETH data sets, the speed are both about 10 fps; for crowded Trecvid 2008 data set, the speed is about 6 fps. Compared with the speed of 7 fps for Trecvid 2008 reported in [8], the online CRF does not add much to the computation cost (detection time costs are not included in either measurement).

6. Conclusion

We described an online CRF framework for multi-target tracking. This CRF considers both global descriptors for distinguishing different targets as well as pairwise descriptors for differentiating difficult pairs. Unlike global descriptors, pairwise motion and appearance models are learned from corresponding difficult pairs, and are further represented by pairwise terms in the CRF energy function. An effective algorithm is introduced to efficiently find associations with low energy, and the experiments show significantly improved results compared with up-to-date methods.

Future improvement can be achieved by adding camera motion inference into pairwise motion models.

Acknowledgments

This paper is based upon work supported in part by Office of Naval Research under grant number N00014-10-1-0517.

References

- [1] National institute of standards and technology: Trecvid 2008 evaluation for surveillance event detection. <http://www.nist.gov/speech/tests/trecvid/2008/>. 5, 6, 8
- [2] A. Andriyenko and K. Schindler. Multi-target tracking by continuous energy minimization. In *CVPR*, 2011. 1, 2, 5, 6, 8
- [3] M. D. Breitenstein, F. Reichlin, B. Leibe, E. Koller-Meier, and L. V. Gool. Online multi-person tracking-by-detection from a single, uncalibrated camera. *IEEE Transactions on Pattern Analysis and Machine Intelligence*, 33(9):1820–1833, 2011. 1, 2
- [4] D. Comaniciu, V. Ramesh, and P. Meer. Real-time tracking of non-rigid objects using mean shift. In *CVPR*, 2000. 2
- [5] A. Ess, K. S. Bastian Leibe, and L. van Gool. Robust multiperson tracking from a mobile platform. *IEEE Transactions on Pattern Analysis and Machine Intelligence*, 31(10):1831–1846, 2009. 5, 6, 8
- [6] M. Isard and A. Blake. Condensation – conditional density propagation for visual tracking. *International Journal of Computer Vision*, 29(1):5–28, 1998. 2
- [7] C.-H. Kuo, C. Huang, and R. Nevatia. Multi-target tracking by online learned discriminative appearance models. In *CVPR*, 2010. 1, 2, 4, 5, 6, 7
- [8] C.-H. Kuo and R. Nevatia. How does person identity recognition help multi-person tracking? In *CVPR*, 2011. 1, 4, 6, 7, 8
- [9] Y. Li, H. Ai, T. Yamashita, S. Lao, and M. Kawade. Tracking in low frame rate video: A cascade particle filter with discriminative observers of different lifespans. In *CVPR*, 2007. 2
- [10] Y. Li, C. Huang, and R. Nevatia. Learning to associate: Hybrid-boosted multi-target tracker for crowded scene. In *CVPR*, 2009. 6
- [11] A. G. A. Perera, C. Srinivas, A. Hoogs, G. Brooksby, and W. Hu. Multi-object tracking through simultaneous long occlusions and split-merge conditions. In *CVPR*, 2006. 1, 2, 5
- [12] H. Pirsiavash, D. Ramanan, and C. C. Fowlkes. Globally-optimal greedy algorithms for tracking a variable number of objects. In *CVPR*, 2011. 1, 2
- [13] H. B. Shitrit, J. Berclaz, F. Fleuret, and P. Fua. Tracking multiple people under global appearance constraints. In *ICCV*, 2011. 1, 2
- [14] B. Song, T.-Y. Jeng, E. Staudt, and A. K. Roy-Chowdhury. A stochastic graph evolution framework for robust multi-target tracking. In *ECCV*, 2010. 2
- [15] S. Stalder, H. Grabner, and L. V. Gool. Cascaded confidence filtering for improved tracking-by-detection. In *ECCV*, 2010. 1, 2
- [16] S. Wang, H. Lu, F. Yang, and M.-H. Yang. Superpixel tracking. In *ICCV*, 2011. 2
- [17] J. Xing, H. Ai, and S. Lao. Multi-object tracking through occlusions by local tracklets filtering and global tracklets association with detection responses. In *CVPR*, 2009. 1, 2
- [18] J. Xing, H. Ai, L. Liu, and S. Lao. Multiple players tracking in sports video: a dual-mode two-way bayesian inference approach with progressive observation modeling. *IEEE Transaction on Image Processing*, 20(6):1652–1667, 2011. 1, 2
- [19] B. Yang, C. Huang, and R. Nevatia. Learning affinities and dependencies for multi-target tracking using a crf model. In *CVPR*, 2011. 1, 2, 4, 6

Method	Recall	Precision	FAF	GT	MT	PT	ML	Frag	IDS
PRIMPT [8]	76.8%	86.6%	0.891	125	58.4%	33.6%	8.0%	23	11
Online CRF Tracking	79.0%	90.4%	0.637	125	68.0%	24.8%	7.2%	19	11

Table 3. Comparison of tracking results on ETH dataset. The human detection results are the same as used in [8], and are provided by courtesy of authors of [8].



Figure 7. Tracking examples on TUD [2], Trecvid 2008 [1], and ETH [5] data sets.